

MYELIN X-RAY PATTERNS RECONCILED

A. E. BLAUROCK

From the MRC Cell Biophysics Unit, Biophysics Department, King's College, London WC2B 5RL, England. Dr. Blaurock's present address is the Department of Chemistry, California Institute of Technology, Pasadena, California 91125.

ABSTRACT Two different X-ray diffraction patterns have been published for frog sciatic myelin. Here the apparent discrepancy is attributed to different spacings between the myelin membranes in the two experiments. Assuming the single membrane has the same structure in the two cases, some restrictions on the phasing are indicated. Several possible profiles for the single membrane are then considered. A profile derived by assuming a lecithin cholesterol-like bilayer within the membrane accounts for all the published data. Three published profiles also are considered. These are not quite in as good agreement with observation, but they cannot be excluded at present.

INTRODUCTION

Although the experimental conditions were strikingly similar, two rather different X-ray diffraction patterns have now been observed from the myelin sheath of frog sciatic nerve in Ringer's solution (1, 2). The differences (Fig. 1 and Table I) are too great to be attributed to experimental error. Because of them, and because of the different methods of analysis, two different profiles have been derived for the single myelin membrane. As a consequence, two distinct bilayer structures have been proposed for the membrane (1, 2).

In this report the differences in the two diffraction patterns are attributed to different distances between neighboring membranes in the respective specimens. An approach is then described to reconcile the two diffraction patterns while assuming the same structure for the single myelin membrane. Several possible profiles are then tested. One of these agrees somewhat better than the others with the two sets of data, but a choice cannot be confidently made. Finally an experiment is proposed which may allow a decisive choice to be made.

DIFFERENCES IN THE PATTERNS

In a recent paper (ref. 1; *I* hereafter), Worthington and McIntosh have described X-ray diffraction experiments on frog sciatic nerve (*Rana pipiens*). However, the data they report are different from those previously reported for frog sciatic nerve (species not given) by Caspar and Kirschner (ref. 2; *II* hereafter): although the myelin had the same periodicity, $D = 171 \text{ \AA}$, prominent differences are seen in Fig. 1 at orders 3, 4, 11, and 12. Other significant differences can be found in Table I. The reader can best confirm the differences by comparing the published densitometer tracings (1, 3). My

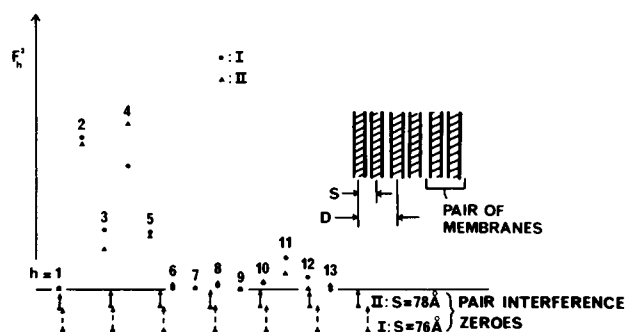


FIGURE 1 The observed F_h^2 values for normal myelin (numerical values given in Table I). A schematic diagram of the repeating structure in myelin is shown to the right. The pair-interference zeroes predicted for the two values of S by assuming a symmetric membrane are indicated by the two rows of arrows below. For an asymmetric membrane, pair-interference zeroes will still be present (see text).

TABLE I
CORRECTED INTENSITIES FROM FROG SCIATIC NERVE
COMPARED WITH PREDICTED VALUES*

h	Observed $F_h^2 \pm \text{error}$		Calculated phase sign and F_h^2			
			Rescaled egg lecithin-cholesterol bilayer†		Best-fit profile§	
	I	II ¶	I**	II ‡	I**	II ‡
1	0.0034 \pm 0.0001	0.0016 \pm 0.0013	+, 0.0005	+, 0.0003	-, 0.0038	-, 0.0012
2	0.3375 \pm 0.0101	0.3232 \pm 0.0092	+, 0.0885	+, 0.0918	+, 0.3269§§	+, 0.3429§§
3	0.1320 \pm 0.0040	0.0890 \pm 0.0096	+, 0.1320	+, 0.0842	+, 0.1318	+, 0.0912
4	0.2737 \pm 0.0082	0.3706 \pm 0.0393	-, 0.4151	-, 0.5075	-, 0.2853	-, 0.3521
5	0.1284 \pm 0.0039	0.1147 \pm 0.0164	-, 0.2170	-, 0.1477	-, 0.1502§§	-, 0.0973§§
6	0.0023 \pm 0.0002	0.0118 \pm 0.0061	+, 0.0099	+, 0.0179	+, 0.0040	+, 0.0094
7	0.0046 \pm 0.0005	0.0032 \pm 0.0023	-, 0.0141	-, 0.0107	-, 0.0064	-, 0.0016
8	0.0076 \pm 0.0008	0.0156 \pm 0.0081	+, 0.0012	+, 0.0079	+, 0.0080	+, 0.0158
9	0.0000	0.000 \pm 0.0008	+, 0.0012	+, 0.0011	0, 0.0001	0, 0.0003
10	0.0125 \pm 0.0013	0.0166 \pm 0.0094	-, 0.0012	+, 0.0015	+, 0.0085	+, 0.0239
11	0.0710 \pm 0.0071	0.0406 \pm 0.0163	+, 0.0976	+, 0.1089	+, 0.0555	+, 0.0538
12	0.0271 \pm 0.0027	0.0020 \pm 0.0014	+, 0.0218	+, 0.0006	+, 0.0196§§	+, 0.0044§§
13	0.00	0.0110 \pm 0.0068	-, 0.0126	-, 0.0202	-, 0.0012	-, 0.0061

* $\sum_{h=1}^{13} F_h^2 = 1.0$.

†Proportionally thickened so that peak-to-peak distance is 44 Å.

§See text for details.

|| Measured on Fig. 3 in ref. 1; error is estimated in ref. 1 as 3% for orders 1–5 and 10% for 6–12. $D = 171$ Å.

¶ Derived from Table I in ref. 2; error is the mean uncertainty in F_h^2 . $D = 170 \pm 1$ Å.

** Assuming $D = 171$ Å and $S = 76$ Å.

‡ Assuming $D = 171$ Å and $S = 78$ Å.

§§ Best-fit values differing from observation by more than the errors determined in ref. 2.

|| || Intensity too weak to detect.

own observations, which have not been reported in detail (but see ref. 4 for a description), agree fairly well with those in *II*.

Pattern *II* also appears to be inconsistent with diffraction patterns from myelin sheath swollen in water and in glycerol solutions (1, 5). In these solutions, layers of fluid form between pairs of membranes. Good agreement of the corrected intensities from the normal myelin with the data from the swollen myelin is expected if the structure of the pair of membranes is not disturbed by the swelling. However, the normal-myelin data in *II* do not fit well with the swollen-myelin data in *I*. Thus the swollen-myelin patterns include a broad band which spans orders 10–13 in the normal pattern, but pattern *II* fits poorly since order 12 is considerably less intense than orders 11 and 13 (Fig. 1). Also, orders 7 and 8 in pattern *II* do not agree particularly well with the swelling data. I note that a similar discrepancy was reported in a previous swelling experiment (6, 7).

From these comparisons I conclude that the pair of membranes has at least two different structures in the various experiments. In the previous swelling experiment, the two membranes in a pair were found to be closer together than normally, i.e., the cytoplasmic space was thinner in the swollen myelin (7).

DETERMINING *S*

In order to find the distances between membranes in the two normal-myelin specimens, I have used the corrected intensities of the first six orders in patterns *I* and *II* to calculate the respective Patterson functions, Fig. 2. From these functions I have determined the center-to-center distance, *S*, between the two membranes in each case (7); *S* is defined in Fig. 1. Given the data in Table I of ref. 2, the distance is $S = 77\frac{3}{4}$ Å, Fig. 2. This is quite close to my reported value, $77\frac{1}{2}$ Å (7). Given the data shown in Fig. 3 of ref. 1, the distance is $S = 76$ Å. The difference, about 2 Å, is small but statistical consideration of the errors in Table I indicates a chance of less than 1% that the difference is insignificant. Assuming a change in *S* by 2 Å, and no other difference, I will show how the two diffraction patterns can be reconciled to within a reasonable experimental error.

CONFIRMING THE DIFFERENT *S*-VALUES

Given a profile of the electron density across the repeating pair of membranes in the myelin sheath, it can be predicted where the phase sign changes from positive to negative, or vice-versa, in the corresponding diffraction pattern. These points are zeroes of diffracted intensity, which define fringes in between. To illustrate, I have assumed that the single membrane is symmetric. In this case certain zeroes are predictable, whatever the shape of the membrane profile. Since these zeroes depend only on the value of *S*, they are called pair-interference zeroes. The arrows in Fig. 1 mark the zeroes for both values of *S*.

In general, when the parts of a structure move closer together, zeroes in the diffraction pattern move away from the origin; and of course the fringes move with them. In

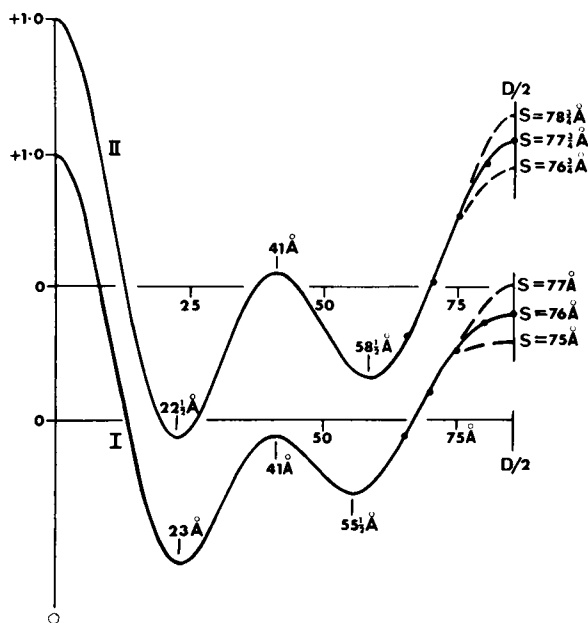


FIGURE 2 The two Patterson functions calculated using the observed F_h^2 values of orders 1–6 in Table I; $D = 171 \text{ \AA}$. Each curve is symmetric about the origin and $D/2$. Near $D/2$ the full circles show the sum of two origin-like peaks (7) centered at S , e.g., 76 \AA , and $D-S$, e.g. 96 \AA . The dashed curves show the effect of varying S by 1 \AA either way.

this way the predicted zeroes in Fig. 1 move to the right when S decreases. For an asymmetric membrane, similar zeroes will occur. Although they will not be at the positions predicted for a symmetric membrane, they will in general shift to the right as S decreases. By comparing the two diffraction patterns in Fig. 1 one can look for the expected shifts as S changes.

In line with the Patterson-function analysis, orders 1–6 in Fig. 1 show the predicted effects of the change in S . Thus when S decreases, the second zero moves away from order 3, which therefore should be more intense in pattern *I* than in *II*. The increase is confirmed in Fig. 1. The second zero moves nearer to order 4, which therefore should be less intense in pattern *I*. The effect is seen in Fig. 1. Similarly, the 5th order is more intense, and the 6th less intense, in pattern *I* than in *II*, as predicted from the decrease in S . The only exception is order 2, which shows a slight increase rather than the slight decrease expected for a decrease in S . I note that ample evidence has already been given for zeroes near order 1, between orders 3 and 4, and between orders 5 and 6 (1, 2, 7–9).

A more rigorous test is afforded by orders 7–13 since these were not used in the Patterson-function analysis. The 7th order is slightly more intense in pattern *I* (Table I), and the 8th less intense, as predicted for a decrease in S . The predicted zero near order 10 in pattern *II* must indeed be to the left of the order: if it were to the right, order 10 would be considerably stronger in pattern *I* than in *II*, contrary to observa-

tion. However, the expected zero in pattern *I* is not necessarily to the right of order 10, and another means is used below to test the phasing. Order 11 should decrease slightly, not increase, as *S* decreases; the discrepancy is attributed to a systematically greater intensity, over orders 10–13, in pattern *I* (see below). Orders 12 and 13 behave as predicted. The zero very near order 12 in pattern *II* could be to either side, but because order 12 is considerably more intense in pattern *I*, the zero in this pattern must be well to the right of the order, as predicted. Both patterns show no measurable intensity at order 9, indicating a nearby minimum in the single-membrane pattern; other evidence for this minimum has been reported (1, 2).

In all, the changes predicted assuming the different values of *S* are fairly well borne out.

The reason for the different values of *S* is not known. Those experimental conditions which are described in both *I* and *II* certainly are the same. I note that changes in *S* have been caused by substituting other media for the Ringer's solution (7).

TESTING POSSIBLE PROFILES

Several possible profiles have been tested against the two diffraction patterns by assuming, first, that the structure of the single membrane is the same in experiments *I* and *II* and, second, that the distance *S* is smaller by 2 Å in *I*.

A Lipid Bilayer-like Profile

The first profile considered was derived by assuming that the myelin membrane contains a bilayer similar to that formed by a mixture of egg lecithin with cholesterol. This assumption is based on the similarities noted in the diffraction patterns from myelin and from the lipid mixture (7, 10), as well as on the lipid composition of myelin (11). The lipid profile is shown in Fig. 3*a* to the same resolution as the myelin data. I note that the profile computed accordingly from my own myelin diffraction data (11) does indeed resemble Fig. 3*a*.

Assuming pairs of the egg lecithin-cholesterol bilayers which are 76 or 78 Å apart, respectively, with water filling the gaps, F_h^2 values and phase signs were calculated. Although the agreement between predicted and observed F_h^2 values was not particularly good, the phase signs predicted for orders 2–6 were those found previously (1, 2, 7–9). Discrepancies in the respective F_h^2 values were attributed both to omitting surface layers of protein (7) from the model—these are expected to affect particularly the first few orders of diffraction (12)—and to a peak-to-peak distance, 42.5 Å in Fig. 3*a*, which is somewhat smaller than the 44–45 Å indicated for the myelin membrane (7, 10). The different distances need to be investigated by recording the diffraction from the extracted myelin lipids. However, as an approximate correction the bilayer thickness was rescaled from 42.5 to 44 Å, and the F_h^2 values and phase signs were recalculated; these are given in Table I under the heading “Rescaled egg lecithin-cholesterol bilayer.” The increase in bilayer thickness brought the F_h^2 values into better agreement with observation, particularly at the higher orders, but the only sign to have changed is that of order 9.

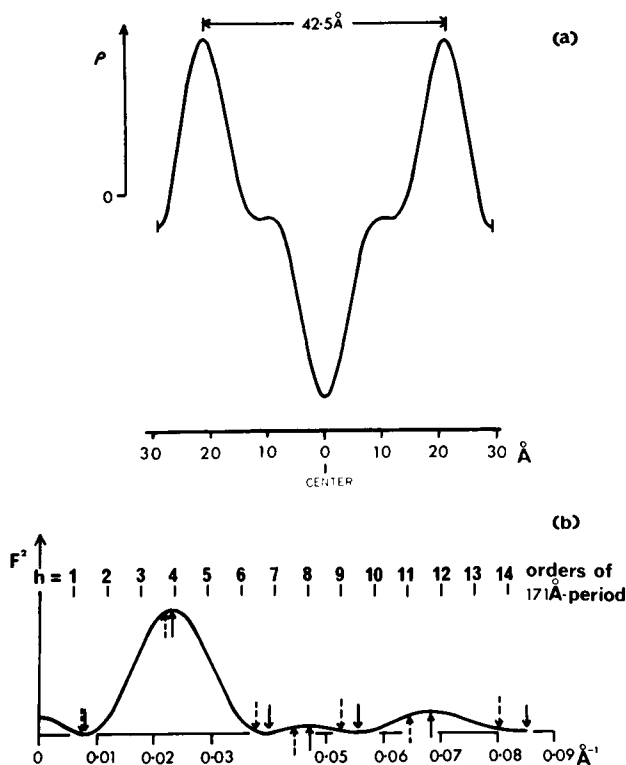


FIGURE 3 (a) The profile of an egg lecithin-cholesterol bilayer (60:40 mol%) calculated using unpublished data kindly supplied by N. P. Franks. The period was 59 Å, and orders 1-4 were used. Much the same profile has been published by Levine and Wilkins (14). (b) The calculated squared Fourier transform. The value for F_0 was estimated from the swelling data of N. P. Franks. Similar diffracted intensity is observed for the lipids dispersed in water (N. P. Franks, unpublished data). The peaks and zeroes are indicated by the solid arrows. For a proportional thickening of the bilayer from 42.5 to 45 Å, the peaks and zeroes will move to the positions of the dashed arrows. The upper row of numbers locates the orders of diffraction from the normal myelin.

Because of the uncertainty, noted above, as to the phasing of order 10 in pattern *I* and of order 12 in *II*, all possible choices of sign for these orders were tested. The signs assumed for the remaining orders are those in Table I under "Rescaled egg lecithin-cholesterol bilayer," excepting order 1 which is widely accepted as negative (1, 2, 7-9). I then calculated the four Fourier syntheses corresponding to the possible signs for the two orders in question. The syntheses showed possible profiles of the pair of membranes. The four single-membrane profiles showed small differences between them, but in appearance they fell into two groups. Next an average profile was computed by summing the two profiles in one group, after the appropriate increase or decrease by 2 Å in the distance S , and the corresponding diffraction pattern of a symmetric pair of the profiles was calculated. The same was done for the other group of two profiles.

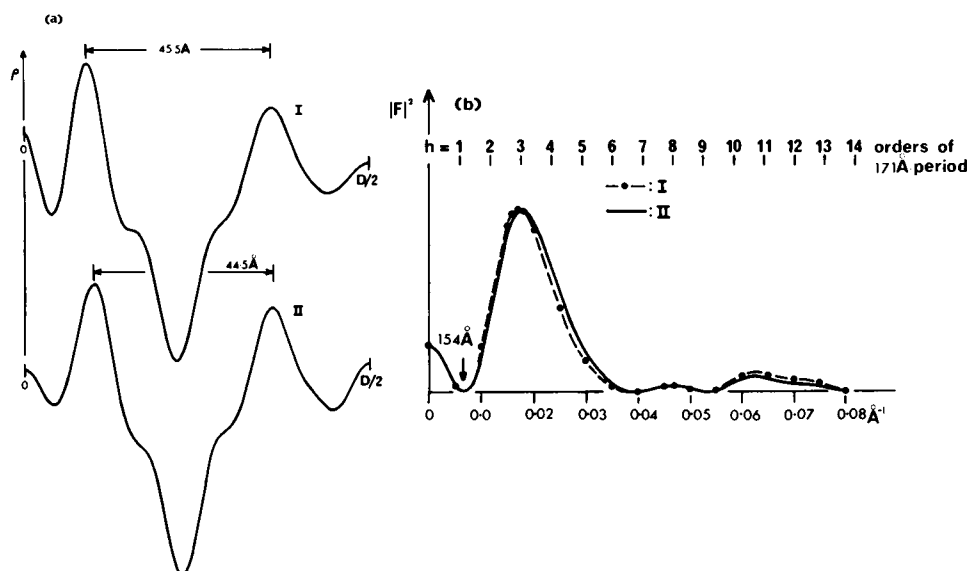


FIGURE 4 (a) The two profiles of the single myelin membrane calculated using the observed $|F_h|$'s and the "best-fit" signs (Table I). The peak at the origin in the upper curve may not correspond to real structure since it is considerably smaller in the lower curve and in my own calculated profile (11). (b) The corresponding squared Fourier transforms of the single-membrane profiles for comparison with Fig. 3b. These curves are expected to differ in detail from those for an isolated myelin membrane since the profile has not been corrected for an apparent overlap with neighboring profiles, as suggested by swelling data (7). The upper row of numbers again locates the orders of diffraction from the normal myelin.

The calculations clearly favored the first group: most of the predicted intensities listed under "Best-fit profile" in Table I agree with the observed values to within the errors determined in II. The few exceptions require somewhat larger errors. Thus, for example, the 2nd order in pattern II needs an error of 6% rather than the more stringent 3% determined in II. The sets of data compared here were measured in two different laboratories, and the agreement appears to be satisfactory.

The two diffraction patterns are reconciled in this way without giving up constant membrane structure.

The two single-membrane profiles calculated from the observed $|F_h|$'s and the best-fit signs are shown in Fig. 4a. Although differences can be picked out, the two profiles compare fairly well.

The profile obtained by averaging the second group (order 10 in I and order 12 in II both negative) gave considerably worse agreement at orders 10 and 12 in both patterns. Nonetheless, it seems premature to rule out this alternative on the basis of the present data.

Other Possible Profiles

The same calculations were repeated on both the preferred and alternative phasings determined by Worthington and McIntosh (I), and on a fourth set, "for completeness."

TABLE II
PREDICTED VALUES* OF F_h^2 BASED ON SOME OTHER PHASINGS,
FOR COMPARISON WITH THE OBSERVED VALUES IN TABLE I

<i>h</i>	W-M preferred†		W-M alternative‡		For completeness	
	<i>I</i>	<i>II</i>	<i>I</i>	<i>II</i>	<i>I</i>	<i>II</i>
1	-, 0.0023	-, 0.0026	-, 0.0031	-, 0.0015	-, 0.0029	-, 0.0022
2	+, 0.3332	+, 0.3281	+, 0.3278§	+, 0.3440§	+, 0.3326	+, 0.3292
3	+, 0.1436§	+, 0.0805	+, 0.1371	+, 0.0887	+, 0.1383	+, 0.0835
4	-, 0.2806	-, 0.3682	-, 0.2861	-, 0.3533	-, 0.2800	-, 0.3696
5	-, 0.1357	-, 0.1116	-, 0.1433	-, 0.1018	-, 0.1425	-, 0.1076
6	+, 0.0050	+, 0.0064	+, 0.0040	+, 0.0094	+, 0.0050	+, 0.0064
7	-, 0.0017§	-, 0.0062§	-, 0.0031	-, 0.0033	-, 0.0043	-, 0.0038
8	-, 0.0112	-, 0.0116	-, 0.0138	-, 0.0068§	+, 0.0102	+, 0.0101
9	0, 0.0000	0, 0.0002	0, 0.0009§	0, 0.0010§	0, 0.0008	0, 0.0008
10	-, 0.0098	-, 0.0218	+, 0.0085	+, 0.0240	-, 0.0098	-, 0.0219
11	-, 0.0563	-, 0.0529	+, 0.0526§	+, 0.0561	-, 0.0532§	-, 0.0552
12	-, 0.0207§	-, 0.0039§	+, 0.0196§	+, 0.0044§	-, 0.0207§	-, 0.0039§
13	0, —	+, 0.0063	0, —	-, 0.0057	0, —	+, 0.0059

* $\sum_{h=1}^{13} F_h^2 = 1.0$.

†Corresponding to the first and second phase choices in ref. 1.

§Values differing from observation by more than the errors determined in ref. 2.

The results are summarized in Table II. The overall agreement between observed and calculated values of F_h^2 is best for the "W-M preferred" and "for completeness" sets. These two sets are in considerably better agreement, overall, than the "best-fit" set in Table I. However, a more detailed comparison tends to support the best-fit set, as follows.

The three sets of phase signs considered in Table II and the best-fit set in Table I differ as to whether there are changes of sign between orders 7 and 8, and between orders 8 and 10 (order 9 being too weak to observe). Comparing the observed data to the four sets of F_h^2 -values, the best agreement at orders 6, 7, and 8 is given by the best-fit set of signs in Table I: only for this set is the ordering of intensities correctly predicted, $6 < 7 < 8$ in pattern *I* and $7 < 6 < 8$ in pattern *II*; and the errors, $\sum_{h=6}^8 |_{\text{obs}} F_h^2 - \text{calc } F_h^2|$, are least for both *I* and *II*. The ordering is stressed because it can be confirmed in the published densitometer tracings (1, 3), which should faithfully reflect the patterns recorded on the X-ray film. Considering orders 6–13, the correct ordering of intensities still is predicted only by the best-fit phasing, and the error is smallest for this set. Thus the calculations are taken on the whole to favor the pair of profiles in Fig. 4a, but a decisive choice is hardly possible.

The respective profiles calculated using the W-M preferred and W-M alternative phasings are shown in Fig. 5. I note that choosing the sign of order 13 in pattern *II* opposite to that of 10–12 always gave better agreement than if orders 10–13 all had the same sign. The dashed curves in Fig. 5 confirm that the agreement is less good in the latter case.

A difficulty in the physical interpretation of Fig. 5a is that the density at the origin,

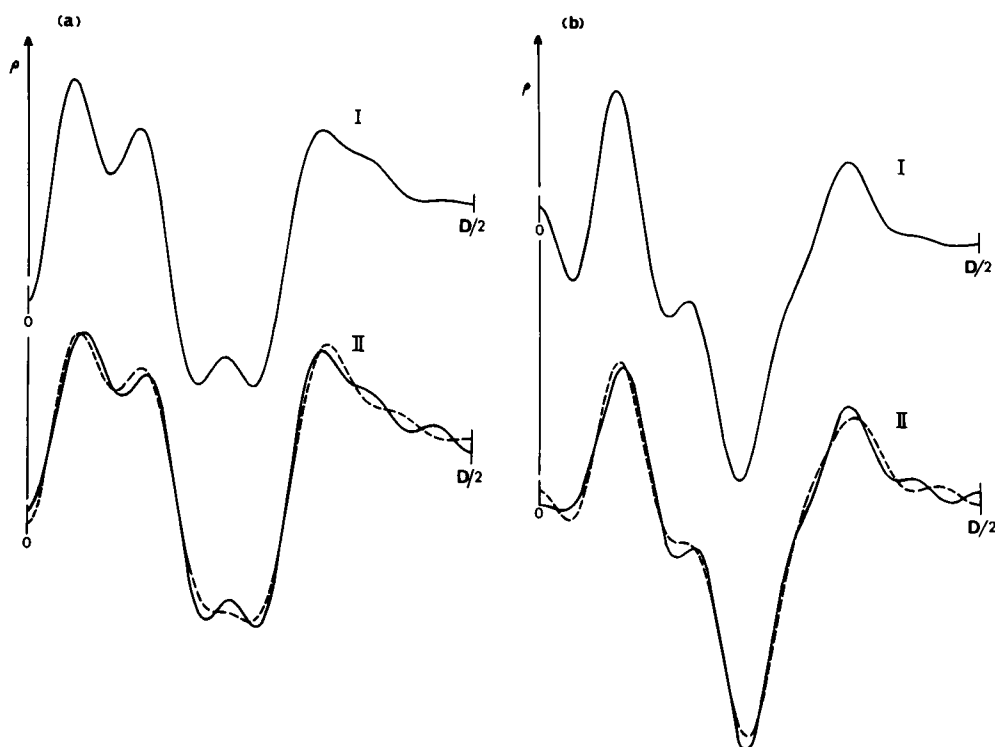


FIGURE 5 Profiles calculated as for Fig. 4a, except that the phase signs are those of the "W-M preferred" (a) or "W-M alternative" (b) sets in Table II. For II, the solid curves were computed assuming that the sign of order 13 is opposite to that of 10–12, while the dashed curves assume the same sign for all these orders.

$0.30 \text{ e}/\text{\AA}^3$ (I), is too low for water, $0.334 \text{ e}/\text{\AA}^3$. A hydrophobic layer—lipid hydrocarbon chains or aliphatic or aromatic amino-acid side chains of the protein in myelin—would account for the low value. However, either interpretation is not consistent with the swelling observed at or very near the origin (7).

DATA FROM SWOLLEN MYELIN

In regard to the myelin sheath swollen in glycerol solutions (1, 5), there is a striking resemblance of the intensity beyond 0.032 \AA^{-1} (see Fig. 1B in I) to the squared Fourier transforms of the single-membrane profiles, Fig. 4b. It is possible to observe the continuous squared transform of the single membrane provided that the spacings between the membranes in all the sheaths vary considerably (13). From the failure to see any trace of Bragg-reflections beyond 0.032 \AA^{-1} , I estimate that the periodicity D varies by $\pm 15 \text{ \AA}$. This variation, and the wide fluid layers in the swollen sheath, make it plausible that S varies. To explain why the zeroes which are predicted in Fig. 1 near orders 8 and 10, and which are confirmed above, are not seen in the swollen-myelin pattern, S would need to vary by $\pm 10 \text{ \AA}$. Systematic changes in S of this size have

been observed in swelling experiments (7). Therefore I suggest that the diffraction from the swollen myelin (1, 5) is, beyond 0.032 \AA^{-1} , mainly the diffraction as though from single myelin membranes.

In *I* the diffraction from the normal sheath agrees fairly well with that from the sheath swollen in glycerol. Nonetheless, I suspect that the agreement is fortuitous beyond 0.032 \AA^{-1} , i.e. that it is due to the particular value of *S* in the normal specimen. A test will be to increase *S* in the swollen myelin to the somewhat larger value found in normal myelin previously (2, 7). The weak order 12 of the normal pattern *II* will then locate a zero nearby in the continuous diffraction from the swollen myelin, if the structure of the pair of membranes is not disturbed.

ANOTHER DIFFERENCE BETWEEN THE TWO NORMAL PATTERNS

The sum of the intensities of the three orders 10, 11, and 12 in pattern *I* is 50% greater than the sum of the four orders 10–13 in *II*. Random errors in measuring intensity are very unlikely to account for this difference. Small differences in the structure of the single membrane cannot be ruled out. Some systematic effects also have been considered, but they cannot be tested conclusively against the data as reported.

The difference suggests a caution against assuming that these data are highly accurate. [See note added in proof.]

CONCLUSION

Of the various profiles considered here, I prefer the “best-fit” profiles shown in Fig. 4*a*. While the present calculations do not rule out some of the others, they do tend to favor an average of the best-fit profiles. The average profile accounts best for the two sets of observed data at just those orders where the phasing is in doubt.

The best-fit profiles are firmly based on a bilayer structure which is known to exist (14). Compared to the egg lecithin-cholesterol bilayer in Fig. 3*a*, both profiles in Fig. 4*a* show the two narrow peaks, identified with the headgroups of the di-acyl lipids, and the narrow trough at the center of the bilayer and shoulders $\pm 10 \text{ \AA}$ from the center, which are a peculiar effect of the cholesterol (10, 14). If confirmed with more accurate data, the differences which are evident—the peaks in the membranes are 2–3 \AA farther apart than in the bilayer and both membranes are somewhat asymmetric—will help in further defining the membrane structure.

Caspar and Kirschner (*II*) have interpreted the profile which they derived by other means, in similar terms. However, in Fig. 4*a* the two shoulders in either profile are considerably nearer the same height than the shoulders in the profile calculated using the slightly different signs put forward in *II*. Assuming the less likely sign for the 10th order in pattern *I*, negative, makes the left shoulder higher than the right one. These observations do not support the asymmetric distribution of the cholesterol that is proposed in *II*.

In view of the limited data, only two sets, and the systematic difference between the two (see above), I have not attempted to derive the best possible profile. Rather I have

limited myself to considering published profiles. For a more rigorous and comprehensive test of the phasing, I suggest experiments in which S is manipulated (7). For small changes in S the membrane structure may not change significantly, and it may be possible to derive a unique set of phase signs. Experiments of this kind have the advantage of comparing two specimens of a single kind of myelinated nerve, rather than comparing, as in *II*, two distinct myelins with different periodicities and different chemical compositions (1, 11).

Note Added in Proof: Our analysis (15) of a myelin diffraction pattern similar to that shown by Kirschner and Caspar (3) indicates that they have wrongly ignored a prominent band of diffuse intensity beneath orders 10–13 in their pattern. Taking the diffuse intensity into account reduces the discrepancy noted above since there is little if any diffuse intensity beneath orders 10–12 in the Worthington-McIntosh pattern (1). The diffuse intensity also needs to be taken into account in order to calculate an accurate profile of the membrane.

I thank Mr. N. P. Franks for unpublished data; Dr. D. S. Gilbert for helpful criticism of an earlier draft; and Ms. Ann Kernaghan for drafting the figures.

Support from the U.S. National Eye Institute (Special Fellowship FO3 EY50584) is gratefully acknowledged.

Received for publication 28 January 1975 and in revised form 16 October 1975.

REFERENCES

1. WORTHINGTON, C. R., and T. J. MCINTOSH. 1974. Direct determination of the lamellar structure of peripheral nerve myelin at moderate resolution (7 Å). *Biophys. J.* **14**:703.
2. CASPAR, D. L. D., and D. A. KIRSCHNER. 1971. Myelin membrane structure at 10 Å resolution. *Nat. New Biol.* **231**:46.
3. KIRSCHNER, D. A., and D. L. D. CASPAR. 1972. Comparative diffraction studies on myelin membranes. *Ann. N. Y. Acad. Sci.* **195**:309.
4. BLAUROCK, A. E., and C. R. WORTHINGTON. 1969. Low-angle X-ray diffraction patterns from a variety of myelinated nerves. *Biochim. Biophys. Acta.* **173**:419–426.
5. WORTHINGTON, C. R., and T. J. MCINTOSH. 1973. Direct determination of the electron density profile of nerve myelin. *Nat. New Biol.* **245**:97.
6. WORTHINGTON, C. R., and A. E. BLAUROCK. 1969. A low-angle X-ray diffraction study of the swelling behaviour of peripheral nerve myelin. *Biochim. Biophys. Acta.* **173**:427.
7. BLAUROCK, A. E. 1971. Structure of the nerve myelin membrane: proof of the low-resolution profile. *J. Mol. Biol.* **56**:35.
8. FINEAN, J. B., and R. E. BURGE. 1963. The determination of the Fourier transform of the myelin layer from a study of swelling phenomena. *J. Mol. Biol.* **7**:672.
9. MOODY, M. F. 1963. X-ray diffraction pattern of nerve myelin: a method for determining the phases. *Science (Wash. D. C.)* **142**:1173.
10. WILKINS, M. H. F., A. E. BLAUROCK, and D. M. ENGELMAN. 1971. Bilayer structure in membranes. *Nat. New Biol.* **230**:72.
11. MOKRASCH, L. C., R. S. BEAR, and F. O. SCHMITT. 1971. Myelin. *Neurosci. Res. Prog. Bull.* **9**:440. (526, for X-ray results; 543, chemical results).
12. BLAUROCK, A. E. 1973. X-ray diffraction pattern from a bilayer with protein outside. *Biophys. J.* **13**:281.
13. HOSEMAN, R., and S. N. BAGCHI. 1962. *Direct Analysis of Diffraction by Matter*. North-Holland Publishing Co., Amsterdam.
14. LEVINE, Y. K., and M. H. F. WILKINS. 1971. Structure of oriented lipid bilayers. *Nat. New Biol.* **230**:69.
15. BLAUROCK, A. E., and J. C. NELANDER. 1976. Disorder in nerve myelin: an analysis of the diffuse X-ray scattering. *J. Mol. Biol.* In press.